Received: 24 June 2019 | Accepted: 28 November 2019

DOI: 10.1111/gcb.14960

PRIMARY RESEARCH ARTICLE

Global Change Biology WILEY

Fluvial CO_2 and CH_4 patterns across wildfire-disturbed ecozones of subarctic Canada: Current status and implications for future change

Ryan H. S. Hutchins[1] | Suzanne E. Tank[1] | David Olefeldt[2] | William L. Quinton[3] | Christopher Spence[4] | Nicole Dion[5] | Cristian Estop-Aragonés[2] | Samson G. Mengistu[1]

[1]Department of Biological Sciences, University of Alberta, Edmonton, AB, Canada

[2]Department of Renewable Resources, University of Alberta, Edmonton, AB, Canada

[3]Cold Regions Research Centre, Wilfrid Laurier University, Waterloo, ON, Canada

[4]National Hydrology Research Centre, Environment and Climate Change Canada, Saskatoon, SK, Canada

[5]Water Resources Department, Government of Northwest Territories, Yellowknife, NT, Canada

Correspondence
Ryan H. S. Hutchins, Department of Biological Sciences, University of Alberta, Edmonton T6G 2E9, Canada.
Email: hutchins.ryan@gmail.com

Present address
Cristian Estop-Aragonés, Ecohydrology and Biogeochemistry Group, Institute of Landscape Ecology, University of Münster, 48149, Münster, Germany

Funding information
Campus Alberta Innovates Program; Northwest Territories Cumulative Impacts Monitoring Program, Grant/Award Number: CIMP180; Polar Knowledge Canada, Grant/Award Number: 1617-0009; Alberta Innovates; NSF-OPP, Grant/Award Number: 1043681, 1559691 and 1542736

Abstract

Despite occupying a small fraction of the landscape, fluvial networks are disproportionately large emitters of CO_2 and CH_4, with the potential to offset terrestrial carbon sinks. Yet the extent of this offset remains uncertain, because current estimates of fluvial emissions often do not integrate beyond individual river reaches and over the entire fluvial network in complex landscapes. Here we studied broad patterns of concentrations and isotopic signatures of CO_2 and CH_4 in 50 streams in the western boreal biome of Canada, across an area of 250,000 km^2. Our study watersheds differ starkly in their geology (sedimentary and shield), permafrost extent (sporadic to extensive discontinuous) and land cover (large variability in lake and wetland extents). We also investigated the effect of wildfire, as half of our study streams drained watersheds affected by megafires that occurred 3 years prior. Similar to other boreal regions, we found that stream CO_2 concentrations were primarily associated with greater terrestrial productivity and warmer climates, and decreased downstream within the fluvial network. No effects of recent wildfire, bedrock geology or land cover composition were found. The isotopic signatures suggested dominance of biogenic CO_2 sources, despite dominant carbonate bedrock in parts of the study region. Fluvial CH_4 concentrations had a high variability which could not be explained by any landscape factors. Estimated fluvial CO_2 emissions were 0.63 (0.09–6.06, 95% CI) and 0.29 (0.17–0.44, 95% CI) g C m^{-2} $year^{-1}$ at the landscape scale using a stream network modelling and a mass balance approach, respectively, a small but potentially important component of the landscape C balance. These fluvial CO_2 emissions are lower than in other northern regions, likely due to a drier climate. Overall, our study suggests that fluvial CO_2 emissions are unlikely to be sensitive to altered fire regimes, but that warming and permafrost thaw will increase emissions significantly.

KEYWORDS

carbon dioxide, CO_2, landscape carbon budgets, methane, permafrost, rivers, streams, wildfires

1 | INTRODUCTION

The boreal biome is a contemporary net carbon sink (Steinkamp & Gruber, 2015), with organic carbon accumulation during the Holocene resulting in this region storing more carbon per unit area than any other biome on Earth (Loisel et al., 2014; Tifafi, Guenet, & Hatté, 2018). A significant fraction of this stored carbon is trapped in permafrost (Hugelius et al., 2014), and thus is largely inaccessible for biogeochemical processing. However, warming in this region (Biskaborn et al., 2019) enables these large carbon stores to become subjected to biogeochemical processing (Pries, Schuur, & Crummer, 2012), by changing hydrologic flow paths (Connon, Devoie, Hayashi, Veness, & Quinton, 2018; Walvoord & Kurylyk, 2016) and enhancing the transport of carbon from land to water (Spence, Kokelj, Kokelj, McCluskie, & Hedstrom, 2015; Toohey, Herman-Mercer, Schuster, Mutter, & Koch, 2016). In addition, increasing air temperatures are causing the boreal region to experience increased wildfire frequency (Coops, Hermosilla, Wulder, White, & Bolton, 2018), which further augments permafrost thaw (Gibson et al., 2018). Thus, permafrost degradation and wildfire act, and interact, to influence carbon mobilization (Robinson & Moore, 2000) by releasing terrestrial carbon stocks to the atmosphere, while also enhancing the lateral transport of carbon from land to aquatic systems (Abbott, Larouche, Jones, Bowden, & Balser, 2014; Dean et al., 2018; Larouche, Abbott, Bowden, & Jones, 2015; Wauthy et al., 2018). However, the effects of these changes on the net carbon balance of affected regions are not well documented.

Coupled with our increased understanding of the importance of land–water carbon transport in northern regions, the importance of aquatic systems as a component of the landscape carbon budget is becoming increasingly recognized (Cole et al., 2007; Drake, Raymond, & Spencer, 2018). Streams and rivers in particular are hotspots of carbon processing and large emitters of carbon to the atmosphere (Raymond et al., 2013) and are closely connected to the terrestrial landscape with carbon from groundwater and soils contributing the vast majority of the carbon pool within fluvial networks (Duvert, Butman, Marx, Ribolzi, & Hutley, 2018; Horgby, Boix Canadell, Ulseth, Vennemann, & Battin, 2019; Lupon et al., 2019; Rasilo, Hutchins, Ruiz-González, & Giorgio, 2017). Fluvial CO_2 emissions could potentially offset land net ecosystem production (NEP, gross primary production minus ecosystem respiration), currently a sink for atmospheric CO_2 (Butman et al., 2016; Lundin et al., 2016), but the proportional importance of these fluxes remains poorly understood in most regions (Webb, Santos, Maher, & Finlay, 2018). In ecosystems affected by wildfire and permafrost thaw, in particular, aquatic offsets of terrestrial net productivity are largely unknown despite evidence pointing to organic matter in permafrost being rapidly mineralized by microbes (Abbott et al., 2014; Drake, Guillemette, et al., 2018; Drake, Wickland, Spencer, McKnight, & Striegl, 2015; Spencer et al., 2015) and thus fuelling CO_2 production in streams. Given the rapid changes occurring in these regions (Callaghan et al., 2010; Rouse et al.., 1997; Schuur et al., 2015), and their relevance to global carbon cycles (Steinkamp & Gruber, 2015), a better understanding of their net ecosystem carbon budgets is clearly required. Only by integrating estimates of terrestrial and aquatic carbon fluxes can net landscape carbon budgets be resolved, and the implications for future change in a warming climate be understood.

In addition to the overall importance of fluvial networks for influencing landscape carbon budgets, headwater streams are increasingly recognized as critical contributors to CO_2 emissions (Marx et al., 2017; Wallin, Löfgren, Erlandsson, & Bishop, 2014), with low order streams shown to dominate atmospheric CO_2 fluxes from inland waters (work in Sweden by Wallin et al., 2018, 2013). Previous work has shown a consistent downstream decline in CO_2 concentrations from headwaters to lower reaches over a vast area of the Eastern Canadian Boreal Shield and Taiga Shield (Hutchins, Prairie, & Giorgio, 2019). However, there are many challenges in estimating emissions from headwaters, including determining the amount of carbon loaded to the stream (Lupon et al., 2019; Rasilo et al., 2017), and difficulties associated with obtaining good-quality direct flux measurements (Marx et al., 2017). Within the Taiga Plains, the drainage network is further complicated by the presence of interconnected bog complexes draining much of the Plains' landscape (Connon, Quinton, Craig, Hanisch, & Sonnentag, 2015), while higher residence time lakes are much more dominant in the Taiga Shield (Spence et al., 2015). Stable carbon isotopes are a tool that has shown promise in estimating CO_2 emissions in headwater streams from a variety of geographic locations (Campeau, Wallin, et al., 2017; Deirmendjian & Abril, 2018; Giesler et al., 2013; Polsenaere & Abril, 2012; Venkiteswaran, Schiff, & Wallin, 2014). Stream network modelling of emissions also has the potential to help resolve headwater emissions (Ågren & Lidberg, 2019; Hutchins, 2019). However, few studies to date have combined stable carbon isotopes and stream network modelling to help resolve watershed CO_2 emissions or compare these approaches.

The Western Canadian Taiga region has several characteristics that render it of interest to study riverine CO_2 and CH_4. Permafrost thaw and increasing wildfire frequency are especially pronounced in the Western Canadian Taiga, which is a subset of the larger boreal biome (Marshall, Schut, & Ballard, 1999). This region has been substantially affected by recent megafires (Walker et al., 2018), while permafrost warming (Biskaborn et al., 2019) has resulted in significant changes in permafrost extent and landscape composition (Carpino, Berg, Quinton, & Adams, 2018; Haynes, Connon, & Quinton, 2018). Compounding these changes, there is evidence that wildfire is accelerating permafrost thaw in this region (Gibson et al., 2018). In turn, these changes can increase basin drainage (Quinton, Hayashi, & Chasmer, 2011) and thus stream flow (Connon, Quinton, Craig, & Hayashi, 2014), which may also increase organic carbon release (O'Donnell et al., 2012). The Western Canadian Taiga is also at the boundary between sporadic and discontinuous permafrost; which has been found to be a region of peak riverine CO_2 emissions elsewhere in the subarctic (Serikova et al., 2018). In addition to the permafrost gradient and wildfire mosaic, this region is characterized by two different ecozones, the Taiga Plains and Taiga Shield. Both ecozones have distinct bedrock, surface deposits,

vegetation and geomorphology, and may thus respond differently to both wildfire and thaw.

In this study, we present a large-scale survey of dissolved gases (CO_2 and CH_4) in streams across the Taiga Plains and Taiga Shield of the Northwest Territories with differing wildfire histories and permafrost regimes. We investigate the landscape drivers of CO_2 and CH_4 in headwater streams and rivers ranging from Strahler order 1–5, and the potential effects of climate and wildfire disturbance. We then estimate CO_2 and CH_4 emissions using both stream network modelling and empirical isotopic mass balance approaches, to place these emissions in the context of other, previously assessed components of the landscape carbon budget (Helbig, Chasmer, Desai, et al., 2017; Helbig, Chasmer, Kljun, et al., 2017; Walker et al., 2018). Finally, we use climate models to assess how these emissions might respond to the rapid changes in climate that are underway within this region.

2 | MATERIALS AND METHODS

2.1 | Sampling and site description

We sampled 50 nonnested first to fifth order streams in summer 2017. The sampling locations were found within two adjacent ecozones of Northwest Territories, Canada: Taiga Plains and Taiga Shield (Marshall et al., 1999), where we sampled 28 and 22 sites respectively (Figure 1a, Tank et al., 2018). Both the Taiga Plains and Shield have a subarctic climate and are part of the greater boreal biome (Brandt, 2009). However, the Shield region is characterized by abundant lakes and by Precambrian bedrock overlain by thin soils, which enables permafrost (where present) to often penetrate to bedrock (Table 1). In the Taiga Shield, most of the streams in the landscape connect lakes and are subject to fill-and-spill hydrology (Spence & Woo, 2003). Peatlands in the Shield occur only in bedrock depressions and are not as widespread as the Taiga Plains where sedimentary deposits are overlain by thick deposits of quaternary sediments. The widespread peatland complexes throughout the Taiga Plains encompass both permafrost affected peat plateaus and nonpermafrost bogs and fens (Connon et al., 2015). In both ecozones, our sample sites included watersheds which were burned and unburned in the 2014 megafires that burned over 28,500 km^2 of the southern Northwest Territories landscape (Figure 1; Walker et al., 2018).

2.2 | Field measurements: Fluvial CO_2 and CH_4 concentrations and isotopes

Water samples for dissolved CO_2 and CH_4 were collected in a 1 L bottle and a headspace of 60 ml was made with ambient air using a syringe. The headspace was equilibrated by shaking the bottle for 2 min and then injected into evacuated vials. Gas from the vials was analysed on a gas chromatograph (Shimadzu GC-8a) for headspace

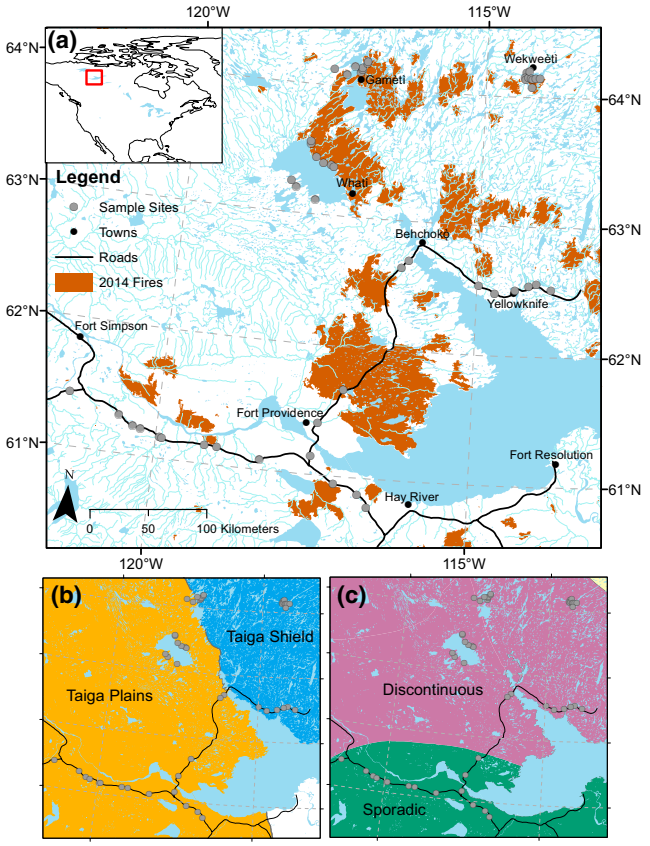

FIGURE 1 Map of the sampled streams and rivers with (a) 2014 fires coverage, and divided into (b) the two ecozones: Taiga Plains and Taiga Shield and c) permafrost extent category (discontinuous and sporadic)

CO_2 and CH_4 concentrations and on a cavity ring down spectrometer (Picarro G2201-i Analyzer) to characterize $\delta^{13}C$. The Picarro analyzer was checked against commercial $\delta^{13}C$-CO_2 standards in each run. Water column concentrations of dissolved CO_2 and CH_4 were calculated using the ambient air concentrations, in situ water temperature, headspace ratio and solubility constants for the two gases (Rumble, Lide, & Bruno, 2018).

2.3 | Field measurements: Velocity and discharge

At each site, velocity was measured at 60% depth at 0.5 m intervals across the channel using a handheld FlowTracker2 (SonTek). The velocity–area method was used to estimate discharge, where velocity was multiplied by the cross-sectional area along each transect with the FlowTracker2 software.

2.4 | Geospatial analyses and statistics

High-resolution digital elevation models (5 m × 5 m) were obtained from ArcticDEM (Porter et al., 2018). Watersheds were delineated with the hydrology toolbox in ArcGIS 10.2, manually corrected if

TABLE 1 Information on streams and their watershed properties (for the Taiga Plains and Taiga Shield ecozones and the overall study area) with summary statistics: medians and quantiles (first, third) in parentheses (median values of percentages may not add up to 100%)

	Unit	Taiga plains	Taiga shield	Both
Latitude	°N	60.8–64.1	62.5–64.2	60.8–64.2
Longitude	°W	116.2–121.5	113.8–117.3	113.8–121.5
Mean annual temperature	°C	−3 to −7	−7	
Mean annual precipitation	mm	225–450	200–300	
Net primary production	g m^2/year	340 (223–405)	210 (194–251)	249 (196–382)
Number of rivers/streams		28	22	50
Strahler orders		1–5	1–5	1–5
Watershed area	km^2	80.5 (25–244)	3.9 (2.1–22.7)	26.5 (3.7–163)
Depth (max)	cm	60 (31–62)	38 (20–62)	46 (30–64)
Width	m	4.3 (2.3–8.3)	1.3 (0.7–3.2)	2.8 (1.3–7.6)
Velocity (mean)	m/s	0.39 (0.29–0.54)	0.09 (0.04–0.19)	0.29 (0.09–0.44)
Discharge	L/s	590 (262–2,279)	33 (8–236)	274 (38–1,260)
Elevation	m	245 (220–265)	216 (211–360)	238 (212–268)
Watershed slope	°	0.5 (0.4–0.8)	3.5 (2.8–4.0)	1.0 (0.4–3.4)
Forest Cover	%	50 (36–59)	45 (20–61)	49 (31–61)
Shrub and Herb	%	3 (5–9)	19 (3–35)	5 (1–17)
Exposed	%	4 (1–10)	9 (3–21)	5 (2–13)
Water	%	6 (2–8)	10 (5–16)	7 (3–13)
Total peatland	%	50 (39–55)	6 (2–10)	28 (9–51)
Perennially frozen peatland	%	31 (23–49)	5 (2–10)	18 (9–40)
Unfrozen peatland	%	11 (8–19)	0 (0–0)	0 (0–11)
Bedrock type		Sedimentary	Metamorphic/volcanic	

needed and the resulting polygons were used to calculate watershed area. Also using the hydrology toolbox, the stream network of each watershed was modelled using the flow accumulation function on the ArcticDEM. Strahler order was calculated on the modelled network. Permafrost extent boundaries were obtained from the National Snow and Ice Data Center (Brown, Ferrians, Heginbottom, & Melnikov, 2002). Geology for each watershed was determined using the Geoscape Canada Maps from GeoGratis (http://geogratis.cgdi.gc.ca/). Additionally, land cover statistics were calculated from the GeoGratis land cover product based on Landsat. Peatland distribution statistics were calculated using the Peatlands of Canada map from Geological Survey of Canada (Tarnocai, Kettles, & Lacelle, 2011). Average net primary production (NPP) for each watershed was obtained from National Aeronautics and Space Administration Moderate Resolution Imaging Spectroradiometer (NASA MODIS) satellite from which average annual NPP was available from 2000 to 2014 (Running & Mu, 2015). All statistics were undertaken using R 3.5 and Model II regression was performed using the *model2* package (Legendre, 2014) using the major axis method. Linear models used to predict CO_2 were identified using ordinary least-square regressions between variables, ±standard error is reported on all coefficients and R^2 values are provided in the R^2-adjusted form. Variables were natural logarithm transformed (log) to improve normality when required (Shapiro–Wilk normality test, $p < .05$). Due to the nonnormal nature of nontransformed data, we report medians and first and third quantiles (25th and 75th percentiles) representing the interquantile range (IQR) since means and standard deviations would be skewed and not robust statistics. Raw data and R code for all calculations are included in the Supporting Information.

2.5 | Broad-scale watershed CO_2 emissions: Stream network modelling

Broad-scale emissions were calculated using two independent approaches: stream network modelling of an idealized drainage network and an empirical isotope mass balance. Both approaches integrate beyond the sampled reaches and provide CO_2 emissions for the entire watershed network upstream of the sampling point. In contrast to fluxes at the reach scale, network emissions take into account the hydrology, configuration and architecture of the network. From a landscape perspective, these modelled integrated emission measures are appropriate

for comparison with other important components of the landscape carbon budget such as terrestrial net ecosystem exchange (NEE).

For the network modelling approach, CO_2 concentrations and emissions were modelled based on contributing area and NPP (see supplemental methods and model results, below). For every stream section in each stream network, discharge, width, slope and velocity were modelled based on empirical relationships from the sampled locations (supplemental methods). Gas transfer velocity (*k*) was calculated using relationships from Natchimuthu, Wallin, Klemedtsson, and Bastviken (2017) based on stream velocity and slope. We chose to use the study by Natchimuthu et al. (2017) because it was designed to explicitly test relationships for prediction of *k*, using measurements from a study region (boreal Scandinavia) that is more similar to our own than other studies. Atmospheric flux (g C/m^2) for each stream section was calculated from modelled CO_2 and *k* and then was multiplied by stream section area (supplemental methods) to provide the total emissions for each section. For the entire stream network in each watershed these emissions were summed and divided by watershed area to provide integrated fluvial emissions of CO_2 per area of landscape. Annual flux rates (g C m^{-2} year^{-1}) were calculated assuming 180 open-water days, following observations from the Water Survey of Canada and by a study at similar latitudes in Alaska (Crawford, Striegl, Wickland, Dornblaser, & Stanley, 2013).

Stream network modelling uncertainty was estimated using Monte Carlo simulation with 1,000 iterations. For each of the models used to calculate stream point hydraulics (i.e. discharge, width, slope and velocity) and CO_2 (supplemental methods), variance–covariance matrices were calculated for each models coefficient, and 1,000 coefficients were generated with the *mnormt* package in R. Gas fluxes were then calculated for each of the sampled watersheds using the modelled range of coefficients and the resulting 5th and 95th percentile confidence interval percentiles were determined. CH_4 was estimated similarly to CO_2 but because there were no significant relationships between CH_4 and any measured parameters (see below), concentrations were not modelled. Instead, Monte Carlo was used to sample the normal distribution of the natural log normalized data at each of 1,000 iterations (similar to Raymond et al., 2013). CH_4 fluxes were calculated in the same manner as CO_2 fluxes using a converted gas exchange coefficient (supplemental methods).

2.6 | Broad-scale watershed CO_2 emissions: CO_2 source and mass balance

Our second approach to estimate broad scale emissions used a mass balance approach with a Miller–Tans plot to estimate the isotopic composition of the source of the dissolved fluvial CO_2, in this case indicating the source of δ^{13}C-CO_2 entering low order streams (Strahler order 1 and 2) from groundwater and/or soil water. Identifying the groundwater source δ^{13}C-CO_2 improves the ability to model CO_2 emissions (Marx et al., 2018) and our approach (back-calculating the source) has the advantage of determining the broad-scale groundwater and soil water δ^{13}C-CO_2 actually entering the stream. In this method, the slope of a model II regression (major axis method) of δ^{13}-CO_2 × CO_2 against CO_2 (more details in Supporting Information) can be used to provide an estimate of the isotopic source signature (Campeau et al., 2018; Campeau, Wallin, et al., 2017; Horgby et al., 2019; Miller & Tans, 2003). Since a Miller–Tans plot does not include processes such as degassing and/or photosynthesis it may yield an inaccurate estimate. To help counter these limitations we only included low order streams. Low order streams represent the start of the aquatic network where the least transformation and degassing of CO_2 have occurred. This calculated source of δ^{13}C-CO_2 was used as an end-member for all sites.

Using the estimated isotopic source value of CO_2 in an empirical degassing trajectory of CO_2 concentration plotted against δ^{13}C-CO_2 (i.e. a regression of observed data), a concentration range of source CO_2 was estimated. From this range of source concentration, CO_2 emissions/loss throughout the stream network (emissions per unit watershed area) was calculated as:

$$CO_2\ \text{loss} = \frac{(CO_{2\,\text{source}} - CO_{2\,\text{stream}}) \times Q \times t}{A}, \quad (1)$$

where $CO_{2\,\text{source}}$ is the source CO_2 concentration, $CO_{2\,\text{stream}}$ is the concentration at the sampling site, *Q* is the discharge (L/s), *t* is a conversion factor from seconds to days (86,400 s/day) and *A* is watershed area (m^2). This method provides a conservative estimate as it does not include any CO_2 produced within the stream. Similar to the network modelling approach, annual flux rates were calculated assuming a 180 day open water season. Stream CO_2 concentrations were binned to watershed area categories <10, 10–100 and >100 km^2, which is representative of the distribution of sites in this study. Mass balance calculations were conducted for each of these bins following the equation above, to enable robust estimates that include uncertainty.

The uncertainty in the mass balance calculation was estimated using Monte Carlo simulation for the modelled sources and Markov chain Monte Carlo (MCMC) for binned stream measurements, both with 10,000 iterations. Briefly, the isotopic source of δ^{13}C-CO_2 (the slope from the Miller–Tans model II regression) was first generated around a normal distribution of the 95% CI of the slope. Next, a variance–covariance matrix was generated for the model coefficients of the empirical degassing relationship (CO_2 concentration vs. δ^{13}C-CO_2). Values for the coefficients were randomly selected around the normal distribution of the variance–covariance matrix 10,000 times using the *mnormt* package in R, and used to calculate the CO_2 source concentration. The resulting modelled source δ^{13}C-CO_2 and CO_2 are reported as 95% confidence intervals of the 10,000 iterations. MCMC sampling was used to quantify uncertainty of binned data. For each of the bins above, MCMC and Gibbs sampling were used to generate 10,000 random samples using the *BEST* package in R. The mass balance for each bin was then calculated 10,000 times using the Monte

Carlo simulated sources and MCMC sampled stream and reported as 95% confidence interval percentiles.

2.7 | Stream CO_2 emissions compared to other components of the landscape carbon balance

A high-resolution estimate of CO_2 emissions from combustion losses during the 2014 megafires was obtained from Walker et al. (2018). Emissions for the delineated watersheds were calculated and expressed per area of watershed and as annual emissions using a fire frequency of 150 years (Coops et al., 2018). NEE of permafrost and nonpermafrost peatland ecosystems was obtained from Helbig, Chasmer, Desai, et al. (2017) who measured and calculated NEE (the additive inverse or opposite sign of NEP) using eddy covariance flux towers. These measurements were made in one of the sampled watersheds in the Taiga Plains. Estimates of peat accumulation were obtained from Loisel et al. (2014) who compiled the information from 268 peat cores across northern peatlands. This time-weighted peat accumulation represents the average rate during the Holocene.

2.8 | Assessing climate impacts on fluvial CO_2 emissions

To assess the potential impact of climate change on fluvial CO_2 emissions, we used scenarios of NPP in future climates, coupled with the empirical model developed here for stream CO_2 concentrations (details in Section 3). For this we used statistically downscaled data from the Pacific Climate Impacts Consortium (PCIC; pacificclimate.org) derived from 12 global climate models for 2051–2080. We used two Representative Concentration Pathway (RCP) scenarios: the medium warming RCP4.5 and the high warming RCP8.5, which correspond to increases in mean annual temperature of 3.1–3.4°C and 4.5–5.0°C, respectively, across the study area. Areas of the Canadian boreal biome with present-day mean annual temperatures analogous to temperatures predicted for our study area display NPP values that are approximately 25% higher for RCP4.5 and 50% higher for RCP8.5. Using these estimates, the above-described stream network modelling exercise was repeated for the study watersheds to estimate potential changes to CO_2 emissions under an increased NPP scenario.

3 | RESULTS

3.1 | Concentrations and isotopic composition across variable landscapes

The sampled streams and rivers were consistently supersaturated in CO_2 and CH_4 throughout both the Taiga Plains and Taiga Shield ecozones. Dissolved CO_2 concentrations spanned an order of magnitude from 0.24 to 4.1 mg C/L with a median of 1.4 (IQR 0.80–2.1) mg C/L or as partial pressure from 421 to 6,044 μatm (median 2,108, IQR 1,420–3,292). Dissolved CH_4 spanned three orders of magnitude from 0.045 to 40 μg C/L with a median of 2.5 (IQR 0.53–6.7) μg C/L or as partial pressure from 1.85 to 1,800 μatm (median 107, IQR 25.5–278). Despite substantial differences in peatland extent, water coverage, stream morphology and bedrock type (Table 1), there was no significant difference in dissolved CO_2 or CH_4 between the Taiga Plains and Taiga Shield (Wilcoxon rank sum test, $p > .5$; Figure 2a; Figure S1a). Additionally, there was no significant difference in either CO_2 or CH_4 from watersheds burned in 2014 and those unburned, both when sites were examined as a whole (Wilcoxon rank sum test, $p > .4$; Figure 2b; Figure S1b), or when other co-occurring factors were taken into account (see below). Dissolved CO_2 was significantly higher in sporadic permafrost areas than in regions of discontinuous permafrost (Wilcoxon rank sum test, $p < .01$; Figure 2c), whereas dissolved CH_4 did not vary significantly with variation in permafrost category (Wilcoxon rank sum test, $p > .9$; Figure S1c). Mean annual watershed NPP (g C m^2 $year^{-1}$) was significantly different between sporadic and discontinuous permafrost

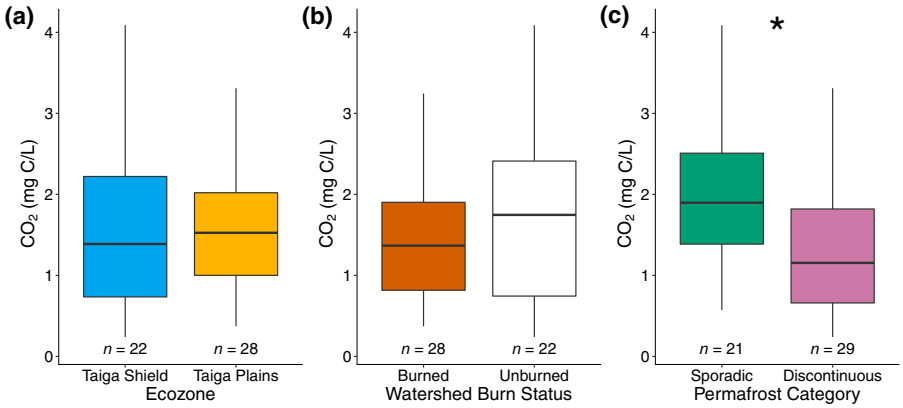

FIGURE 2 Boxplots of dissolved CO_2 concentrations in the sampled streams and rivers separated by different features of the landscape mosaic: (a) the two ecozones Taiga Shield and Taiga Plains, (b) watersheds affected by the 2014 wildfires (burned) and unaffected (unburned) and (c) permafrost extent category (discontinuous and sporadic). Boxplots show the median, first and third quartiles, and whiskers extend to the furthest data point that is within 1.5 times the interquartile range. Asterisk (*) indicates significant difference (Wilcoxon rank sum test, $p < .01$)

TABLE 2 Linear regressions predicting CO_2 concentrations (mg C/L) and $\delta^{13}C$-CO_2 (‰), where Net Primary Production (NPP) is in g C m^2/year, watershed area (area) is in km^2, order is Strahler stream order (unitless), and permafrost extent: Sporadic = 1 and Discontinuous = 0

	Equation	*p*	R^2	*n*
(2)	$\log(CO_2) = 0.00322 \pm 0.00086 \times NPP - 0.626 \pm 0.254$	<.001	0.21	50
(3)	$\log(CO_2) = -0.139 \pm 0.037 \times \log(area) + 2.66 \pm 0.150$	<.001	0.21	50
(4)	$\log(CO_2) = -0.231 \pm 0.059 \times order + 0.935 \pm 0.189$	<.001	0.23	50
(5)	$\log(CO_2) = 0.744 \pm 0.138 \times (permafrost\ extent) - 0.184 \pm 0.031 \times \log(area) + 3.112 \pm 0.520$	<.0001	0.50	50
(6)	$\log(CO_2) = 0.00418 \pm 0.00065 \times NPP - 0.181 \pm 0.0285 \times \log(area) - 0.286 \pm 0.196$	<.001	0.56	50
(7)	$\delta^{13}C\text{-}CO_2 = 0.810 \pm 0.171 \times \log(area) - 21.52 \pm 0.69$	<.0001	0.30	50
(8)	$\log(CO_2) = -0.151 \pm 0.020 \times \delta^{13}C\text{-}CO_2 - 2.56 \pm 0.383$	<.0001	0.50	50

Note: All coefficients listed with ±*SE*.

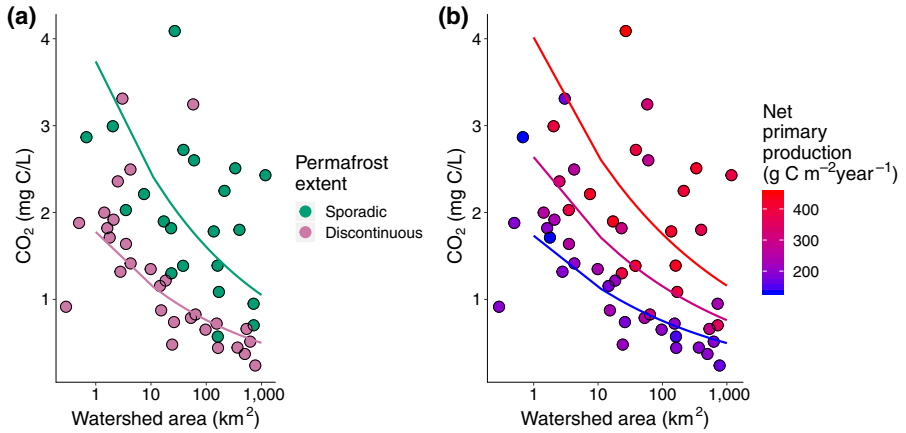

FIGURE 3 Plots of dissolved CO_2 concentrations (mg C/L) and watershed area (km^2, on a $\log_{10}$ axis) with a) points coloured with categories of permafrost extent and lines showing CO_2 predicted from a linear model with watershed area and permafrost extent (where Sporadic = 1 and Discontinuous = 0), $\log(CO_2) = 0.744 \times (permafrost\ extent) - 0.184 \times \log(area) + 0.575$, $R^2 = .50$, $n = 50$, $p < .0001$, (b) with points showing watershed net primary production (NPP, from NASA MODIS years 2000–2014 averaged), $\log(CO_2) = 0.00418 \times NPP - 0.181 \times \log(area) - 0.286$, $R^2 = .56$, $n = 50$, $p < .0001$. CO_2 concentrations decline down the fluvial networks and are modulated by climate (permafrost/NPP)

categories (Wilcoxon rank sum test, $p < .001$; Table 1) and in addition to the relationship between CO_2 and permafrost category, higher watershed NPP was related to higher CO_2 (Table 2, Equation 2). Concentrations of dissolved CO_2 declined with both watershed area in km^2 (Table 2, Equation 3) and Strahler stream order (Table 2, Equation 4). Combined in a linear model, watershed area and permafrost category explained half of the variation in dissolved CO_2 in the studied streams (Table 2, Equation 5, Figure 3a). Permafrost category and NPP were highly related, however, NPP is a continuous variable and a linear model with both watershed area and NPP showing that NPP was more predictive of CO_2 than the permafrost category (Table 2, Equation 6, Figure 3b). There was a lack of relationship between CO_2 and ecozone, fire extent, latitude, land cover, elevation and slope even using multivariate regressions. In contrast to CO_2, there were no significant relationships between CH_4 and landscape characteristics.

Dissolved $\delta^{13}C$-CO_2 in the studied streams ranged from −24.2 to −8.9‰ with a median value of −19.3 (IQR: −21.0 to −17.0). There was no significant difference in dissolved $\delta^{13}C$-CO_2 between streams underlain by carbonate-containing bedrock of the Taiga Plains and those underlain by the poorly weatherable igneous and metamorphic bedrock characterizing the Taiga Shield (Wilcoxon rank sum test, $p > .5$; Figure S2a). In contrast, dissolved bicarbonate, Mg and Ca were all significantly higher in the Taiga Plains than in the Taiga Shield (Wilcoxon rank sum test, $p < .00001$; Figure S3). Additionally, the relationship between dissolved bicarbonate and $\delta^{13}C$-CO_2 was very weak ($R^2 = .06$, $p = .048$). There were also no significant differences between $\delta^{13}C$-CO_2 and 2014 burn status (Wilcoxon rank sum test, $p > .05$; Figure S2b) or categorical permafrost extent (Wilcoxon rank sum test, $p > .05$; Figure S2c). There was a positive relationship between $\delta^{13}C$-CO_2 and watershed area, with $\delta^{13}C$-CO_2 becoming more enriched with increasing area

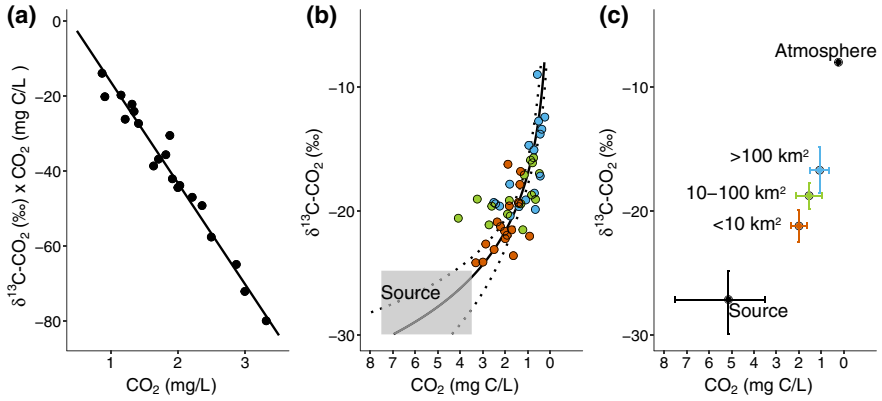

FIGURE 4 Relationships between δ^{13}C-CO_2 and CO_2 throughout the fluvial networks (a) Miller–Tans plot showing δ^{13}C-CO_2 × CO_2 and CO_2 concentration of low order streams where line is model II regression (major axis method): δ^{13}C-CO_2 × CO_2 = −27.1 × CO_2 − 11.01, n = 20, R^2 = .97, and the slope (−27.1, 95% CI: −29.9 to −24.8) represents the source signature, (b) Empirical degassing trajectory of δ^{13}C-CO_2 against CO_2 throughout the sampled streams log(CO_2) = −0.151 × δ^{13}C-CO_2 − 2.56, n = 50, R^2 = .53 with the dotted line representing 95% CI of the regression, (c) The continuum of CO_2 and δ^{13}C-CO_2 from the source (median and 95% CI from (a) and (b), see Section 2), medians and 95% CI of each bin of watershed area (●<10 km^2, ●10–100 km^2 and ●>100 km^2) from Markov chain Monte Carlo sampling of stream measurements with the atmosphere indicated

(Table 2, Equation 7; Figure S4): A Miller–Tans plot of δ^{13}C-CO_2 × CO_2 and CO_2 concentration of low order streams (Figure 4a) showed a slope of −27.1 (95% CI: −29.9 to −24.8, Figure 4a) ‰. There was a negative relationship between δ^{13}C-CO_2 and CO_2 (Table 2, Equation 8, Figure 4b), with δ^{13}C-CO_2 becoming more enriched with lower CO_2 (p < .0001). Using a normal distribution of the slope around the 95% CI from the Miller–Tans plot in the Monte Carlo regression of δ^{13}C-CO_2 against CO_2 (see Section 2, above) resulted in a calculated source CO_2 concentration of 5.1 (95% CI: 3.5 to 7.5, Figure 4c) mg C/L. MCMC sampling of watershed size-binned stream CO_2 concentrations resulted in concentrations of 2.0 (95% CI: 1.7–2.4) mg C/L for watersheds <10 km^2, 1.6 (95% CI: 1.0–2.2) mg C/L for watershed 10–100 km^2, and 1.1 (95% CI: 0.7–1.5) mg C/L for watersheds >100 km^2. Similarly, δ^{13}C-CO_2 of the streams were −22.5 (95% CI: −22.5 to −19.8) ‰ for watersheds <10 km^2, −18.8 (95% CI: −19.8 to −17.7) ‰ for watersheds 10–100 km^2 and −16.7 (95% CI: −18.5 to −14.9) ‰ for watersheds >100 km^2 (Figure 4c). The CO_2 concentrations from the source and three watershed categories in the stream network were used in a mass balance to estimate CO_2 fluxes from streams in the region.

Dissolved δ^{13}C-CH_4 in the studied streams ranged from −66.8 to −44.1‰ with a median of −55.0 (IQR: −58.6 to −51.7). Unlike δ^{13}C-CO_2 and CO_2, there was no relationship between δ^{13}C-CH_4 and CH_4 concentration (p > .1; Figure S5). Additionally, there were no significant differences in δ^{13}C-CH_4 between ecozone (Wilcoxon rank sum test, p > .05), 2014 burn status (Wilcoxon rank sum test, p > .9) or permafrost extent category (Wilcoxon rank sum test, p > .1) and no trend with watershed area (p > .9).

3.2 | Emissions estimates

The two approaches used to estimate CO_2 emissions, stream network modelling and mass balance, yielded similar median CO_2 emissions estimates. Stream network modelling of the sampled watersheds resulted in median CO_2 emission estimates of 0.63 g C m^{-2} year^{-1} (0.09–6.06 g C m^{-2} year^{-1}; 5th and 95th confidence interval percentiles; Monte Carlo simulation) per area of the watershed landscape. Similarly, the mass balance calculation of CO_2 emissions resulted in a median estimate of 0.29 g C m^{-2} year^{-1} (0.17–0.44 g C m^{-2} year^{-1}; 5th and 95th confidence interval percentiles). Median mass balance estimates were similar across the watershed size bins, with 0.28 for <10 km^2, 0.30 for 10–100 km^2 and 0.32 for >100 km^2, all expressed as g C m^{-2} year^{-1} per area of watershed landscape (5th and 95th confidence interval percentiles of 0.14–0.50, 0.15–0.50 and 0.18–0.51 respectively). Applying CH_4 to the stream network modelling exercise resulted in CH_4 emissions estimates three orders of magnitude lower than those for CO_2, at 0.53 mg C m^{-2} year^{-1} (0.095–7.0; 5th and 95th confidence interval percentiles). Studies also often report fluxes per area of stream per day; based on stream network modelling CO_2 flux was 3.2 g C m^{-2} day^{-1} (0.42–61; 5th and 95th confidence interval percentiles) and CH_4 flux was 2.8 mg C m^{-2} day^{-1} (0.49–63).

4 | DISCUSSION

Neither the stark differences in ecozone characteristics (i.e. variation in geomorphology, geology and vegetation between the Taiga Plains and Taiga Shield) nor wildfire history across our study area of approximately a quarter of million square kilometres could account for the observed variation in CO_2 and CH_4 concentration and emission. Instead, extent of permafrost, remotely sensed net primary productivity and watershed size were the main drivers of stream CO_2 concentrations. Conversely, CH_4 concentrations showed no clear patterns relative to any of the landscape properties or water chemistry parameters that were assessed. Our two approaches for estimating CO_2 emissions gave reasonably consistent results allowing us to extrapolate with some confidence across our study region, and compare these vertical fluxes

with other, previously calculated components of this region's net ecosystem carbon balance. Below, we discuss in more detail the drivers of CO_2 and CH_4 across this subarctic landscape, and discuss the importance of stream efflux within the broader carbon balance of this region both today, and under future climate scenarios.

4.1 | Controls on fluvial CO_2 and CH_4 across a discontinuous permafrost landscape

Our sampling occurred 3 years after the 2014 megafires. Consequently, we cannot preclude that wildfire had a transient effect on CO_2 emission that was no longer present at the time of sampling. We are unaware of other studies in the boreal biome that have investigated the effect of wildfire on fluvial CO_2 and CH_4 concentrations, but several studies have assessed the impact of wildfire on stream and lake dissolved organic carbon (DOC) concentrations and export. For example, a study from Alaska found that wildfire and associated permafrost collapse had limited impact on stream DOC 4 years postfire (Larouche et al., 2015). Studies in boreal lakes have found varying impacts from wildfire, with decreases (Betts & Jones, 2009), increases (Carignan, D'Arcy, & Lamontagne, 2000; McEachern, Prepas, Gibson, & Dinsmore, 2000) and no effects (Marchand, Prairie, & Giorgio, 2009; Olefeldt, Devito, & Turetsky, 2013) on DOC concentration. There is increasing evidence that both CO_2 and DOC in streams originate mainly from adjacent water-saturated soils, and are transported from there into stream waters, with DOC undergoing transformation to CO_2 throughout the riparian to downstream corridor (Hutchins et al., 2017; Ledesma et al., 2017; Leith et al., 2015; Öquist, Wallin, Seibert, Bishop, & Laudon, 2009; Rasilo et al., 2017). Observations and models of burn extent for the same wildfires that affected our study watersheds show the wettest areas of the landscape, including riparian zones, and had substantially lower proportions of combustion (Walker et al., 2018). Therefore, it seems likely that the main generators of DOC and CO_2 within the western Canadian Taiga landscape may not have been substantially affected by wildfire over the short- to medium-term time scales encapsulated by this study (Burd et al., 2018). This conclusion is further reinforced by the Tans–Miller-determined $\delta^{13}C$-CO_2 source (mean = 27.1‰, Figure 2c) which is also strongly suggestive of CO_2 originating from soil respiration and/or degradation of terrigenous DOC. Given additional recent evidence that the source of CO_2 in small streams is atmospheric C that was fixed by vegetation during the previous growing season (Campeau et al., 2019), and previous observations from our study streams that DOC is predominately modern despite old DOC in peatland porewater (Burd et al., 2018), it seems likely that wildfire—in this region at least—has either a very transient, or no effect on CO_2 generation over the time scale of one to several years.

The climatic and network position controls on stream water CO_2 are not unique to the western Canadian subarctic. A general decline in CO_2 with network position is well-established in the northern hemisphere (Butman & Raymond, 2011; Campeau, Lapierre, Vachon, Giorgio, & a., 2014; Crawford et al., 2013; Humborg et al., 2010; Teodoru, Giorgio, Prairie, & Camire, 2009; Wallin et al., 2018) but there is also significant heterogeneity confounding this pattern (Duvert et al., 2018; Rocher-Ros, Sponseller, Lidberg, Mörth, & Giesler, 2019). In this study, the rate of CO_2 decline downstream is greatest in the headwaters, and plateaus in larger rivers. To better understand these mechanisms of decline, we calculated the first-order gas loss (Chapra & Di Toro, 1991), a measure of the distance length of reach over which 95% of the gases are dissipated from diffusive mixing. The first-order gas loss was on average 41 km in our study area but, despite the downstream decline in CO_2, it could take as much as 8,400 km to reach equilibrium with the atmosphere based on our empirical models (Figure S14). CO_2 supersaturation in streams and rivers is ubiquitous (Raymond et al., 2013) and in spite of general downstream decline and degassing, CO_2 may never reach equilibrium with the atmosphere because of constant inputs and internal production (Hotchkiss et al., 2015). Recently, climatic variables (such as NPP) have also been linked to the lateral export of carbon in fluvial networks (Magin, Somlai-Haase, Schäfer, & Lorke, 2017; Stackpoole et al., 2017) as well as directly to fluvial dissolved carbon concentrations at a large scale (Hutchins et al., 2019).

Here the patterns of fluvial CO_2 concentrations are parallel to those from the eastern Canadian Boreal and Taiga Shield regions (Hutchins et al., 2019), where CO_2 concentrations have also been shown to increase with increasing NPP and consistently decline downstream. However, the eastern Canadian Boreal and Taiga regions have either no, or limited permafrost (Brown et al., 2002), and higher runoff (Statistics Canada, 2017) and lower soil organic carbon stocks (Hugelius et al., 2014) compared with the area of this study. Additionally, we find similar responses across our two ecozones, despite clear differences in runoff regimes and carbon storage between them. Given all these factors are known to affect carbon transport from land to water (Li Yung Lung et al., 2018), it seems likely that network position, and NPP, are overarching factors that govern subarctic CO_2 dynamics, even in settings with contrasting geology and geomorphology. However, we do note that NPP and network position only explained half of the variation in CO_2 in our analyses, indicating that local drivers also control CO_2 concentrations at smaller scales.

In addition to the lack of differences in CO_2 concentrations between the Taiga Plains and Shield, there was also no significant difference in $\delta^{13}C$-CO_2 between these two regions. Given the carbonate containing bedrock of the Plains and the high bicarbonate concentrations from our study streams in this region (median 160, IQR: 98 to 200 mg/L) compared to the Shield (median 27, IQR: 20 to 37 mg/L), the lack of differences in $\delta^{13}C$-CO_2 is a surprising result (Figure S3a). Our calculated source $\delta^{13}C$-CO_2 signature for both regions was −27.1‰ (95% CI: −29.9 to −24.8) which is consistent with C3 plants (−29 to −24‰, O'Leary, 1988) and therefore indicative of a biogenic rather than geogenic source from mineral weathering. Similar to our findings, a $\delta^{13}C$-CO_2 study from an alpine stream network in Switzerland found that the main source of CO_2 was soil respiration despite the presence of carbonate bedrock and geogenic DIC (Horgby et al., 2019). Additionally, a study in Sweden using $\delta^{13}C$-DIC (whereas we measured $\delta^{13}C$-CO_2) found that DIC was mainly

biogenic, but that a geogenic influence was present in watersheds with carbonate bedrock (Campeau, Wallin, et al., 2017). Also using δ^{13}C-DIC, CO_2 has been shown to be mainly biogenic in Australia (Duvert et al., 2019), where soils have 10-fold lower soil organic carbon content than those in our study region (Tifafi et al., 2018). Our results suggest that CO_2 is mainly biogenic in origin across large expanses of the western Canadian subarctic. This is in agreement with a large-scale interregional comparison (Hutchins et al., 2019) that found CO_2 was controlled by climatic factors across regions, while DIC was controlled by geology. The recent study in alpine Switzerland even suggests that CO_2 is not in equilibrium with DIC based on paired δ^{13}C-CO_2 and δ^{13}C-DIC measurements (Horgby et al., 2019). More research is required to understand these discrepancies but direct δ^{13}C-CO_2 measurements may be required to properly evaluate the source of CO_2 in fluvial networks.

The modelled source CO_2 concentrations had a large 95% CI ranging from 3.5 to 7.5 mg/L potentially indicating large heterogeneity in sources. The magnitude and heterogeneity in source CO_2 is consistent with measured soil and groundwater in boreal regions. For example, within a single hillslope shallow porewater CO_2 varied from 4.6 ± 2.0 mg/L in mineral upland soils to 17.7 ± 3.5 mg/L in organic-rich riparian soils in a Swedish old growth forest (Campeau et al., 2019). Across study regions, measured soil CO_2 can vary greatly from as high as 36.5 ± 21.8 mg/L in peatland soils in Sweden (Campeau et al., 2019) and as low as 2.5 ± 0.3 mg/L in riparian soils in Quebec (Rasilo et al., 2017). At small scales it is possible to track source CO_2 delivered to the stream by monitoring hydrological transects (i.e. Campeau et al., 2019; Öquist et al., 2009), however, it is unclear how these hillslope processes scale to larger watersheds and regions with diverse hydrological connectivity. Given the large heterogeneity and the difficulty in determining the contribution from diverse sources, reconstructing a large-scale degassing trajectory can help constrain the regional CO_2 source to rivers and streams.

Throughout the studied fluvial networks, CH_4 was supersaturated relative to the atmosphere as has been widely reported in the literature (Billett & Harvey, 2012; Campeau & del Giorgio, 2014; Crawford et al., 2014, 2013; Hope, Palmer, Billett, & Dawson, 2001; Huotari, Nykänen, Forsius, & Arvola, 2013; Hutchins et al., 2019; Kling, Kipphut, & Miller, 1992; Striegl, Dornblaser, McDonald, Rover, & Stets, 2012; Wallin et al., 2018). Here there was no relationship between fluvial CH_4 and CO_2 ($p > .2$), whereas several studies have reported correlations between the two (Campeau & del Giorgio, 2014; Crawford et al., 2014; Hutchins et al., 2019; Rasilo et al., 2017; Stanley et al., 2016; Wallin et al., 2018). In contrast to fluvial CO_2, CH_4 showed no patterns with any landscape properties. This suggests that CH_4 may be controlled by local properties rather than the watershed landscape. However, we found that no local explanatory variables were able to predict CH_4 except for a small effect of stream depth ($R^2 = .08$, $p = .03$). While dissolved CH_4 concentration spanned three orders of magnitude, dissolved δ^{13}C-CH_4 showed less variation around a median of −55.0 (IQR: −58.6 to −51.7)‰. Few studies have measured δ^{13}C-CH_4 in streams, however, a recent study from alpine Switzerland with similar values as ours shows that acetoclastic pathways from adjacent soils are likely the source of stream CH_4 (Flury & Ulseth, 2019). Additionally, it has been suggested that fluvial CH_4 concentrations are influenced by available local organic matter (Crawford et al., 2017; Romeijn, Comer-Warner, Ullah, Hannah, & Krause, 2019; Stanley et al., 2016). However, the Taiga Plains captured in our study area has among the highest organic carbon stocks on Earth (Tifafi et al., 2018), suggesting that carbon limitation serves unlikely as a broad, underlying mechanism for the observed CH_4 concentrations and δ^{13}C-CH_4 at the scale of our study. Therefore, factors controlling fluvial CH_4 concentrations and resulting emissions in this region are cryptic and require additional study.

4.2 | Estimates of fluvial CO_2 and CH_4 emissions

The stream network modelling and empirical mass balance showed similar fluvial CO_2 emissions (expressed per unit watershed area) of 0.63 g C m^{-2} $year^{-1}$ (0.09–6.06) and 0.29 g C m^{-2} $year^{-1}$ (0.17–0.44) respectively. This is a notable coherence given the difference in overall approach and underlying rationale for the methods. Despite this similarity, estimates from stream network modelling were generally higher than for the mass balance. There are several possibilities for this difference; the mass balance does not take into account internal production of CO_2 throughout the stream network which has been observed by others (Hotchkiss et al., 2015; Hutchins et al., 2017; Rocher-Ros, Sponseller, Bergström, Myrstener, & Giesler, 2019) and may therefore underestimate emissions. Another possibility is the stream network emissions were overestimated since the gas exchange was modelled using relationships developed in Sweden (Natchimuthu et al., 2017), and may not reflect the conditions in the western Canadian Taiga. Additionally, the modelled drainage network is idealized and therefore does not capture the true complexity of the interconnected bogs draining the landscape in the Taiga Plains (Connon et al., 2015) or lakes of the Taiga Shield (Spence & Woo, 2003). For example, bogs in the Plains are drained by wide slow-flowing channel fens with complex geometry (Quinton, Hayashi, & Pietroniro, 2003) and the stream network model routes simplified channels regardless of landscape type.

Across our study watersheds, stream network modelled CO_2 emissions were negatively correlated to average watershed slope (Figure S15c; Spearman's $\rho = -0.43$), and positively correlated with wetland coverage (Figure S15f; Spearman's rho = 0.47). Measures of allometry (watershed size and stream area) had little effect on overall emissions, despite being included in models to predict CO_2 concentration. Surprisingly, NPP showed only a small positive correlation with total CO_2 emissions (Figure S15d, Spearman's $\rho = 0.25$). Additionally, there was no correlation with lake coverage (Figure S15e; Spearman's $\rho = -0.07$). Although there is significant uncertainty in model estimates at the watershed scale, which limits our ability to parse out between-catchment correlations, it seems that watershed slope and the related wetland extent may have a relatively pronounced impact on watershed-scale emissions, and that NPP may have a more modest effect. As a whole, these estimates also provide a constraint on

the magnitude of regional emissions, enabling comparison with other components of the landscape carbon budget, as described in the section below.

The emissions estimates reported here are similar to a headwater stream network in interior Alaska (0.44 g C m^{-2} $year^{-1}$; 95% CI: 0.08–1.22) which contained discontinuous permafrost in a similar proportion to our study area (Crawford et al., 2013). Similarly, a recent study in the continuous permafrost region of the Northwest Territories found emissions approximately 0.4 g C m^{-2} $year^{-1}$ per watershed landscape area (Zolkos, Tank, Striegl, & Kokelj, 2019). In contrast, large-scale studies in Alaska estimated much higher emissions of 9.0 g C m^{-2} $year^{-1}$ (Striegl et al., 2012) and 7.0 g C m^{-2} $year^{-1}$ (Stackpoole et al., 2017) for boreal portions of the Yukon River. Much of Alaska may not be comparable to the western Canadian Taiga, however, as parts of Alaska have much greater topographic relief and warmer, wetter climates. Additionally, emissions estimates from studies in Québec (1.0–4.6 g C m^{-2} $year^{-1}$; Campeau & del Giorgio, 2014; Hutchins et al., 2019; Teodoru et al., 2009) and Sweden (1.6–8.6 g C m^{-2} $year^{-1}$; Humborg et al., 2010; Jonsson et al., 2007; Lundin, Giesler, Persson, Thompson, & Karlsson, 2013; Wallin et al., 2011, 2018) were somewhat higher than the estimates from this study, but also in areas of very different climate, geomorphology, soils and permafrost extent. In particular, our study region has significantly lower precipitation (200–400 mm) compared to Québec (700–1,000 mm) and Sweden (650–1,250 mm). Thus, the western Canadian Taiga has significantly less runoff generation and stream network area likely causing lower emissions estimates despite similar CO_2 concentrations. Based on the contrasting emissions estimates across high latitudes, it is clear that individual regions have distinct properties resulting in different magnitudes of emissions. In our study area, the drivers of CO_2 concentrations (NPP and network position) are very similar to those in other boreal regions (Hutchins et al., 2019) but landscape fluvial emissions are the result of a complex interplay between stream network architecture and gas exchange which are poorly understood (Ulseth et al., 2019; Wallin et al., 2018). Future work should focus on developing cross-regional relationships of the broad and overarching controls on fluvial emissions in the landscape.

4.3 | Incorporating streams within the landscape: Emissions in the context of watershed-scale carbon budgets

Few studies have integrated fluvial CO_2 emissions with other components of the landscape carbon budget (Butman et al., 2016; Campeau, Bishop, et al., 2017; Campeau, Wallin, et al., 2017; Webb et al., 2018). To better understand the importance of our vertical flux estimates to the landscape carbon balance and consider fluvial emissions in the context of wildfire emissions and terrestrial NEE (Helbig, Chasmer, Kljun, et al., 2017; Turner, Jacobson, Ritts, Wang, & Nemani, 2013; Walker et al., 2018), we used previously published models and measurements from within our study area to assess the net ecosystem carbon balance of the western

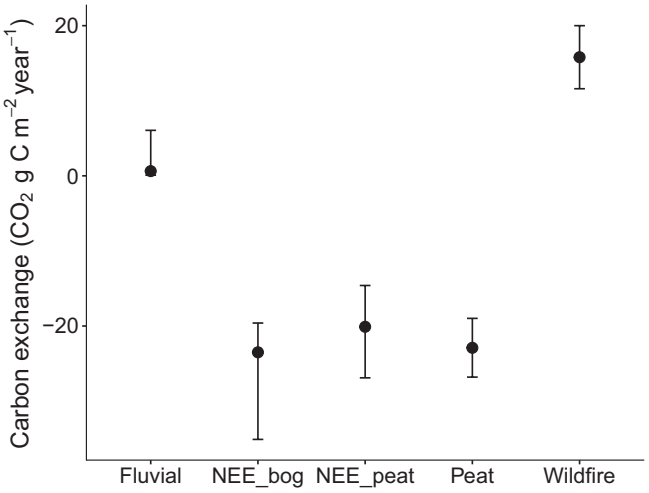

FIGURE 5 Plot of components of the landscape carbon budget: fluvial emissions from stream network modelling, net ecosystem exchange from eddy covariance flux towers for permafrost peatlands (NEE_peat) and nonpermafrost peatlands (NEE_bog) from Helbig, Chasmer, Desai, et al. (2017), Holocene peat accumulation from peat cores Loisel et al. (2014), and 2014 wildfire emissions (Walker et al., 2018) per watershed area normalized to 150 year fire cycle (Coops et al., 2018)

Canadian Taiga. Our estimates of landscape fluvial CO_2 emissions in the western Taiga Shield and Plains are overall low compared to both permafrost and nonpermafrost peatland NEE measured in the Taiga Plains by eddy covariance, and 2014 wildfire emissions modelled for the Taiga Shield and Plains (Figure 5). Northern Holocene peat accumulation rates (−22.9 g C m^{-2} $year^{-1}$; 95% CI: −22.9 to −19.0) were very similar to nonpermafrost bog NEE measured by eddy covariance (−23.5 g C m m^{-2} $year^{-1}$; 95% CI: −25.1 to −19.6). Wildfire combustive emissions, assuming a 150 year fire cycle (+15.8 g C m^{-2} $year^{-1}$; 95% CI: 11.6 to 20.0) were large enough to offset much of the permafrost peatland NEE (−20.1 g C m^{-2} $year^{-1}$; 95% CI: −26.9 to −14.6).

Although fluvial emissions are small, the difference between fire emissions and the permafrost peatland forest sink is only −4.3 g C m^{-2} $year^{-1}$, with uncertainty in both directions. Several factors suggest that these NEE estimates may be somewhat high for our study landscape as a whole. First, the eddy covariance measurements available for this assessment are specifically from peatlands in the Taiga Plains; different land cover types such as upland forest (which has extensive coverage in both of our studied ecozones) might have lower NEE. Additionally, the Taiga Shield has extensive bedrock outcrops and exposed land that would be a negligible carbon sink, suggesting that fluvial emissions may represent a larger fraction of the landscape carbon balance in this area. Modelled NEE by Turner et al. (2013) for all of North America includes wildfire emissions and gives a range of NEE over broader landscape types. Using this NEE map of North America, our study watersheds displayed an average of −24 g C m^{-2} $year^{-1}$ (range: +22 to −68). Thus, our credible range in fluvial emissions (0.09–6.06 g C m^{-2} $year^{-1}$) has the potential to offset potential landscape carbon

sinks. This is compounded by the fact that we have not considered ponds and lakes in our estimates, which occupy a median 7% of our study catchments (35-fold the area occupied by streams), and have generally been shown to be emitters of CO_2 to the atmosphere in northern regions (Bogard & del Giorgio, 2016; Holgerson & Raymond, 2016; Kokic, Wallin, Chmiel, Denfeld, & Sobek, 2015; Raymond et al., 2013; but see Bogard et al., 2019; Tank, Lesack, & Hesslein, 2009). Given that wildfire emissions may overtake the peatland forest sink with increasing wildfire frequency and severity (Coogan, Robinne, Jain, & Flannigan, 2019; Harden et al., 2000), it seems clear that aquatic emissions are important components that could regulate the carbon balance of subarctic landscape, and should therefore be considered in future scenarios of landscape and climate change.

4.4 | Potential responses of the landscape C budget to a changing climate

There are rapid changes occurring throughout the boreal biome, with significant implications for the global carbon cycle. Yet, net landscape carbon budgets and, in particular, the net carbon balance in future climates, is poorly understood for these regions. As discussed above, our study region likely acts as a present-day net carbon sink depending on the fire frequency. However, it is unclear how this landscape will respond to rapid changes and the effect that these changes may have on the carbon balance. In both moderate (RCP4.5) and high (RCP8.5) warming scenarios, the net terrestrial landscape carbon uptake is projected to potentially reverse by the end of the century. The resulting increases in ecosystem respiration are projected to outweigh increasing gross primary production by 25 ± 14 and 103 ± 38 g C m^{-2} $year^{-1}$ for moderate and high warming respectively (Helbig, Chasmer, Desai, et al., 2017). We project stream CO_2 emissions to increase from an estimated 0.63–0.84 g C m^{-2} $year^{-1}$ under moderate warming and to 1.11 g C m^{-2} $year^{-1}$ under high warming, during 2051–2080. This corresponds to a 77% increase in stream CO_2 emissions for an estimated 50% increase in NPP in the high warming scenario. It should be noted that changes in runoff generation could further alter these emissions with higher flows favouring emissions, but these scenarios were not considered here. However, these projections indicate that a greater proportion of fixed CO_2 may be emitted from streams as climate warms, further offsetting current sinks, and adding to the projected increases in ecosystem respiration and wildfire emissions across this region. Thus, across a variety of ecosystem components, it appears that the trajectory of the western Canadian Taiga carbon balance is poised to shift from a net carbon sink to a carbon source in the coming decades with climate change, with fluvial emissions further enhancing this trend.

ACKNOWLEDGEMENTS

This research would not have occurred without the assistance of community directors and local guides in the Tłı̨cho communities of Whatì, Gamètì and Wekweètì (April Alexis, Shirley Dokum, Gloria Ekendia-Gon, Adeline Football, Lloyd Bishop, Alfred Arrowmaker and William Quitte). We additionally thank Erin MacDonald and Luke Gjini for logistical and field support, and acknowledge funding support from the Northwest Territories Cumulative Impacts Monitoring Program (CIMP; grant CIMP180), Polar Knowledge Canada (grant 1617-0009) and the Campus Alberta Innovates Program. DEMs provided by the Polar Geospatial Center under NSF-OPP awards 1043681, 1559691, and 1542736. The authors have no conflicts of interest to declare.

ORCID

Ryan H. S. Hutchins https://orcid.org/0000-0002-1696-4934
Suzanne E. Tank https://orcid.org/0000-0002-5371-6577
David Olefeldt https://orcid.org/0000-0002-5976-1475
Cristian Estop-Aragonés https://orcid.org/0000-0003-3231-9967

REFERENCES

Abbott, B. W., Larouche, J. R., Jones, J. B., Bowden, W. B., & Balser, A. W. (2014). Elevated dissolved organic carbon biodegradability from thawing and collapsing permafrost. *Journal of Geophysical Research: Biogeosciences*, *119*(10), 2049–2063.

Ågren, A. M., & Lidberg, W. (2019). The importance of better mapping of stream networks using high resolution digital elevation models; upscaling from watershed scale to regional and national scales. *Hydrology and Earth System Sciences Discussions*, February, 1–20. https://doi.org/10.5194/hess-2019-34

Betts, E. F., & Jones, J. B. (2009). Impact of wildfire on stream nutrient chemistry and ecosystem metabolism in boreal forest catchments of interior Alaska. *Arctic, Antarctic, and Alpine Research*, *41*(4), 407–417.

Billett, M. F., & Harvey, F. H. (2012). Measurements of CO_2 and CH_4 evasion from UK peatland headwater streams. *Biogeochemistry*, *114*(1–3), 165–181.

Biskaborn, B. K., Smith, S. L., Noetzli, J., Matthes, H., Vieira, G., Streletskiy, D. A., … Lantuit, H. (2019). Permafrost is warming at a global scale. *Nature Communications*, *10*(1), 264.

Bogard, M. J., & del Giorgio, P. A. (2016). The role of metabolism in modulating CO_2 fluxes in boreal lakes. *Global Biogeochemical Cycles*, *30*(10), 1509–1525.

Bogard, M. J., Kuhn, C. D., Johnston, S. E., Striegl, R. G., Holtgrieve, G. W., Dornblaser, M. M., … Butman, D. E. (2019). Negligible cycling of terrestrial carbon in many lakes of the arid circumpolar landscape. *Nature Geoscience*, *12*(3), 180–185.

Brandt, J. (2009). The extent of the North American boreal zone. *Environmental Reviews*, *17*(NA), 101–161.

Brown, J., Ferrians, O., Heginbottom, J. A., & Melnikov, E. (2002). *Circum-Arctic map of permafrost and ground-ice conditions, version 2*. Boulder, CO: National Snow and Ice Data Center.

Burd, K., Tank, S. E., Dion, N., Quinton, W. L., Spence, C., Tanentzap, A. J., & Olefeldt, D. (2018). Seasonal shifts in export of DOC and nutrients from burned and unburned peatland-rich catchments, Northwest Territories. *Canada. Hydrology and Earth System Sciences*, *22*(8), 4455–4472.

Butman, D., & Raymond, P. A. (2011). Significant efflux of carbon dioxide from streams and rivers in the United States. *Nature Geoscience*, *4*(12), 839–842.

Butman, D., Stackpoole, S., Stets, E., McDonald, C. P., Clow, D. W., & Striegl, R. G. (2016). Aquatic carbon cycling in the conterminous United States and implications for terrestrial carbon accounting. *Proceedings of the National Academy of Sciences of the United States of America*, *113*(1), 58–63.

Callaghan, T. V., Bergholm, F., Christensen, T. R., Jonasson, C., Kokfelt, U., & Johansson, M. (2010). A new climate era in the sub-Arctic: Accelerating climate changes and multiple impacts. *Geophysical Research Letters*, *37*(14), 1–6.

Campeau, A., Bishop, K., Amvrosiadi, N., Billett, M. F., Garnett, M. H., Laudon, H., … Wallin, M. B. (2019). Current forest carbon fixation fuels stream CO_2 emissions. *Nature Communications*, *10*(1), 1876.

Campeau, A., Bishop, K. H., Billett, M. F., Garnett, M. H., Laudon, H., Leach, J. A., … Wallin, M. B. (2017). Aquatic export of young dissolved and gaseous carbon from a pristine boreal fen: Implications for peat carbon stock stability. *Global Change Biology*, *23*(4), 5523–5536. https://doi.org/10.1111/gcb.13815

Campeau, A., Bishop, K., Nilsson, M. B., Klemedtsson, L., Laudon, H., Leith, F. I., … Wallin, M. B. (2018). Stable carbon isotopes reveal soil-stream DIC linkages in contrasting headwater catchments. *Journal of Geophysical Research: Biogeosciences*, 1–19.

Campeau, A., & Del Giorgio, P. A. (2014). Patterns in CH_4 and CO_2 concentrations across boreal rivers: Major drivers and implications for fluvial greenhouse emissions under climate change scenarios. *Global Change Biology*, *20*(4), 1075–1088. https://doi.org/10.1111/gcb.12479

Campeau, A., Lapierre, J.-F., Vachon, D., del Giorgio, P. A. (2014). Regional contribution of CO_2 and CH_4 fluxes from the fluvial network in a lowland boreal landscape of Québec. *Global Biogeochemical Cycles*, *28*(1), 57–69.

Campeau, A., Wallin, M. B., Giesler, R., Löfgren, S., Mörth, C.-M., Schiff, S., … Bishop, K. (2017). Multiple sources and sinks of dissolved inorganic carbon across Swedish streams, refocusing the lens of stable C isotopes. *Scientific Reports*, *7*(1), 9158.

Carignan, R., D'Arcy, P., & Lamontagne, S. (2000). Comparative impacts of fire and forest harvesting on water quality in Boreal Shield lakes. *Canadian Journal of Fisheries and Aquatic Sciences*, *57*(S2), 105–117.

Carpino, O. A., Berg, A. A., Quinton, W. L., & Adams, J. R. (2018). Climate change and permafrost thaw-induced boreal forest loss in northwestern Canada. *Environmental Research Letters*, *13*(8), 084018.

Chapra, S. C., & Di Toro, D. M. (1991). Delta method for estimating primary production, respiration, and reaeration in streams. *Journal of Environmental Engineering*, *117*(5), 640–655.

Cole, J. J., Prairie, Y. T., Caraco, N. F., McDowell, W. H., Tranvik, L. J., Striegl, R. G., … Melack, J. (2007). Plumbing the global carbon cycle: Integrating inland waters into the terrestrial carbon budget. *Ecosystems*, *10*(1), 172–185.

Connon, R., Devoie, É., Hayashi, M., Veness, T., & Quinton, W. (2018). The influence of shallow taliks on permafrost thaw and active layer dynamics in subarctic Canada. *Journal of Geophysical Research: Earth Surface*, *123*(2), 281–297.

Connon, R. F., Quinton, W. L., Craig, J. R., Hanisch, J., & Sonnentag, O. (2015). The hydrology of interconnected bog complexes in discontinuous permafrost terrains. *Hydrological Processes*, *29*(18), 3831–3847.

Connon, R. F., Quinton, W. L., Craig, J. R., & Hayashi, M. (2014). Changing hydrologic connectivity due to permafrost thaw in the lower Liard River valley, NWT. *Canada*. *Hydrological Processes*, *28*(14), 4163–4178.

Coogan, S., Robinne, F.-N., Jain, P., & Flannigan, M. (2019). Scientists' warning on wildfire – A Canadian perspective. *Canadian Journal of Forest Research*.

Coops, N. C., Hermosilla, T., Wulder, M. A., White, J. C., & Bolton, D. K. (2018). A thirty year, fine-scale, characterization of area burned in Canadian forests shows evidence of regionally increasing trends in the last decade. *PLoS ONE*, *13*(5), e0197218.

Crawford, J. T., Loken, L. C., West, W. E., Crary, B., Spawn, S. A., Gubbins, N., … Stanley, E. H. (2017). Spatial heterogeneity of within-stream methane concentrations. *Journal of Geophysical Research: Biogeosciences*, *122*(5), 1036–1048.

Crawford, J. T., Lottig, N. R., Stanley, E. H., Walker, J. F., Hanson, P. C., Finlay, J. C., & Striegl, R. G. (2014). CO_2 and CH_4 emissions from streams in a lake-rich landscape: Patterns, controls, and regional significance. *Global Biogeochemical Cycles*, *28*(3), 197–210.

Crawford, J. T., Striegl, R. G., Wickland, K. P., Dornblaser, M. M., & Stanley, E. H. (2013). Emissions of carbon dioxide and methane from a headwater stream network of interior Alaska. *Journal of Geophysical Research: Biogeosciences*, *118*(2), 482–494.

Dean, J. F., Van Der Velde, Y., Garnett, M. H., Dinsmore, K. J., Baxter, R., Lessels, J. S., … Billett, M. F. (2018). Abundant pre-industrial carbon detected in Canadian Arctic headwaters: Implications for the permafrost carbon feedback. *Environmental Research Letters*, *13*(3).

Deirmendjian, L., & Abril, G. (2018). Carbon dioxide degassing at the groundwater-stream-atmosphere interface: Isotopic equilibration and hydrological mass balance in a sandy watershed. *Journal of Hydrology*, *558*, 129–143.

Drake, T. W., Guillemette, F., Hemingway, J. D., Chanton, J. P., Podgorski, D. C., Zimov, N. S., & Spencer, R. G. M. (2018). The ephemeral signature of permafrost carbon in an arctic fluvial network. *Journal of Geophysical Research: Biogeosciences*, *123*(5), 1475–1485.

Drake, T. W., Raymond, P. A., & Spencer, R. G. M. (2018). Terrestrial carbon inputs to inland waters: A current synthesis of estimates and uncertainty. *Limnology and Oceanography Letters*, *3*(3), 132–142.

Drake, T. W., Wickland, K. P., Spencer, R. G. M., McKnight, D. M., & Striegl, R. G. (2015). Ancient low-molecular-weight organic acids in permafrost fuel rapid carbon dioxide production upon thaw. *Proceedings of the National Academy of Sciences of the United States of America*, *112*(45), 13946–13951.

Duvert, C., Bossa, M., Tyler, K. J., Wynn, J. G., Munksgaard, N. C., Bird, M. I., … Hutley, L. B. (2019). Groundwater-derived DIC and carbonate buffering enhance fluvial CO_2 evasion in two Australian tropical rivers. *Journal of Geophysical Research: Biogeosciences*, *124*(2), 312–327.

Duvert, C., Butman, D. E., Marx, A., Ribolzi, O., & Hutley, L. B. (2018). CO_2 evasion along streams driven by groundwater inputs and geomorphic controls. *Nature Geoscience*, *11*, 813–818.

Flury, S., & Ulseth, A. (2019). Exploring the sources of unexpected high methane concentrations and fluxes from Alpine headwater streams. *Geophysical Research Letters*, *46*, 6614–6625. https://doi.org/10.1029/2019GL082428

Gibson, C. M., Chasmer, L. E., Thompson, D. K., Quinton, W. L., Flannigan, M. D., & Olefeldt, D. (2018). Wildfire as a major driver of recent permafrost thaw in boreal peatlands. *Nature Communications*, *9*(1). https://doi.org/10.1038/s41467-018-05457-1

Giesler, R., Mörth, C.-M., Karlsson, J., Lundin, E. J., Lyon, S. W., & Humborg, C. (2013). Spatiotemporal variations of pCO_2 and δ^{13}C-DIC in subarctic streams in northern Sweden. *Global Biogeochemical Cycles*, *27*(1), 176–186.

Harden, J. W., Trumbore, S. E., Stocks, B. J., Hirsch, A., Gower, S. T., O'neill, K. P., & Kasischke, E. S. (2000). The role of fire in the boreal carbon budget. *Global Change Biology*, *6*(S1), 174–184. https://doi.org/10.1046/j.1365-2486.2000.06019.x

Haynes, K. M., Connon, R. F., & Quinton, W. L. (2018). Permafrost thaw induced drying of wetlands at Scotty Creek, NWT, Canada. *Environmental Research Letters*, *13*(11), 114001.

Helbig, M., Chasmer, L. E., Desai, A. R., Kljun, N., Quinton, W. L., & Sonnentag, O. (2017). Direct and indirect climate change effects on carbon dioxide fluxes in a thawing boreal forest-wetland landscape. *Global Change Biology*, *23*(8), 3231–3248. https://doi.org/10.1111/gcb.13638

Helbig, M., Chasmer, L. E., Kljun, N., Quinton, W. L., Treat, C. C., & Sonnentag, O. (2017). The positive net radiative greenhouse gas forcing of increasing methane emissions from a thawing boreal forest-wetland landscape. *Global Change Biology*, *23*(6), 2413–2427. https://doi.org/10.1111/gcb.13520

Holgerson, M. A., & Raymond, P. A. (2016). Large contribution to inland water CO_2 and CH_4 emissions from very small ponds. *Nature Geoscience*, *9*(3), 222–226.

Hope, D., Palmer, S. M., Billett, M. F., & Dawson, J. J. C. (2001). Carbon dioxide and methane evasion from a temperate peatland stream. *Limnology and Oceanography*, *46*(4), 847–857.

Horgby, Å., Boix Canadell, M., Ulseth, A. J., Vennemann, T. W., & Battin, T. J. (2019). High-resolution spatial sampling identifies groundwater as driver of CO_2 dynamics in an Alpine stream network. *Journal of Geophysical Research: Biogeosciences*, https://doi.org/10.1029/2019JG005047

Hotchkiss, E. R., Hall, R. O. Jr, Sponseller, R. A., Butman, D., Klaminder, J., Laudon, H., … Karlsson, J. (2015). Sources of and processes controlling CO_2 emissions change with the size of streams and rivers. *Nature Geoscience*, *8*(9), 696–699.

Hugelius, G., Strauss, J., Zubrzycki, S., Harden, J. W., Schuur, E. A., Ping, C. L., … Kuhry, P. (2014). Estimated stocks of circumpolar permafrost carbon with quantified uncertainty ranges and identified data gaps. *Biogeosciences*, *11*(23), 6573–6593.

Humborg, C., Mörth, C.-M., Sundbom, M., Borg, H., Blenckner, T., Giesler, R., & Ittekkot, V. (2010). CO_2 supersaturation along the aquatic conduit in Swedish watersheds as constrained by terrestrial respiration, aquatic respiration and weathering. *Global Change Biology*, *16*(7), 1966–1978. https://doi.org/10.1111/j.1365-2486.2009.02092.x

Huotari, J., Nykänen, H., Forsius, M., & Arvola, L. (2013). Effect of catchment characteristics on aquatic carbon export from a boreal catchment and its importance in regional carbon cycling. *Global Change Biology*, *19*(12), 3607–3620. https://doi.org/10.1111/gcb.12333

Hutchins, R. (2019). *Incorporation of greenhouse gas emission dynamics from boreal rivers into the global carbon cycle*. PhD thesis, Université du Québec à Montréal. Retrieved from https://archipel.uqam.ca/12416/

Hutchins, R. H. S., Aukes, P., Schiff, S. L., Dittmar, T., Prairie, Y. T., & del Giorgio, P. A. (2017). The optical, chemical, and molecular dissolved organic matter succession along a boreal soil-stream-river continuum. *Journal of Geophysical Research: Biogeosciences*, https://doi.org/10.1002/2017JG004094

Hutchins, R. H. S., Prairie, Y. T., & del Giorgio, P. A. (2019). Large-scale landscape drivers of CO_2, CH_4, DOC and DIC in boreal river networks. *Global Biogeochemical Cycles*, *33*(2), 125–142. https://doi.org/10.1029/2018GB006106

Jonsson, A., Algesten, G., Bergström, A. K., Bishop, K., Sobek, S., Tranvik, L. J., & Jansson, M. (2007). Integrating aquatic carbon fluxes in a boreal catchment carbon budget. *Journal of Hydrology*, *334*(1–2), 141–150. https://doi.org/10.1016/j.jhydrol.2006.10.003

Kling, G. W., Kipphut, G. W., & Miller, M. C. (1992). The flux of CO_2 and CH_4 from lakes and rivers in arctic Alaska. *Hydrobiologia*, *240*(1–3), 23–36.

Kokic, J., Wallin, M. B., Chmiel, H. E., Denfeld, B. A., & Sobek, S. (2015). Carbon dioxide evasion from headwater systems strongly contributes to the total export of carbon from a small boreal lake catchment. *Journal of Geophysical Research: Biogeosciences*, *120*(1), 13–28. https://doi.org/10.1002/2014JG002706

Larouche, J. R., Abbott, B. W., Bowden, W. B., & Jones, J. B. (2015). The role of watershed characteristics, permafrost thaw, and wildfire on dissolved organic carbon biodegradability and water chemistry in Arctic headwater streams. *Biogeosciences*, *12*(14), 4221–4233.

Ledesma, J. L. J., Futter, M. N., Blackburn, M., Lidman, F., Grabs, T., Sponseller, R. A., … Köhler, S. J. (2017). Towards an improved conceptualization of riparian zones in boreal forest headwaters. *Ecosystems*, 1–19. https://doi.org/10.1007/s10021-017-0149-5

Legendre, P. (2014). Model II regression user's guide, R edition. Retrieved from Cran.R-Project.Org, *4*, 1–14.

Leith, F. I., Dinsmore, K. J., Wallin, M. B., Billett, M. F., Heal, K. V., Laudon, H., … Bishop, K. (2015). Carbon dioxide transport across the hillslope–riparian–stream continuum in a boreal headwater catchment. *Biogeosciences*, *12*(6), 1881–1892.

Li Yung Lung, J. Y. S., Tank, S. E., Spence, C., Yang, D., Bonsal, B., McClelland, J. W., & Holmes, R. M. (2018). Seasonal and geographic variation in dissolved carbon biogeochemistry of rivers draining to the Canadian Arctic Ocean and Hudson Bay. *Journal of Geophysical Research: Biogeosciences*, *123*(10), 3371–3386. https://doi.org/10.1029/2018JG004659

Loisel, J., Yu, Z., Beilman, D. W., Camill, P., Alm, J., Amesbury, M. J., … Zhou, W. (2014). A database and synthesis of northern peatland soil properties and Holocene carbon and nitrogen accumulation. *Holocene*, *24*(9), 1028–1042.

Lundin, E. J., Giesler, R., Persson, A., Thompson, M. S., & Karlsson, J. (2013). Integrating carbon emissions from lakes and streams in a subarctic catchment. *Journal of Geophysical Research: Biogeosciences*, *118*(3), 1200–1207. https://doi.org/10.1002/jgrg.20092

Lundin, E. J., Klaminder, J., Giesler, R., Persson, A., Olefeldt, D., Heliasz, M., … Karlsson, J. (2016). Is the subarctic landscape still a carbon sink? Evidence from a detailed catchment balance. *Geophysical Research Letters*, *43*(5), 1988–1995.

Lupon, A., Denfeld, B. A., Laudon, H., Leach, J., Karlsson, J., & Sponseller, R. A. (2019). Groundwater inflows control patterns and sources of greenhouse gas emissions from streams. *Limnology and Oceanography*, *64*(4), 1545–1557. https://doi.org/10.1002/lno.11134

Magin, K., Somlai-Haase, C., Schäfer, R. B., & Lorke, A. (2017). Regional-scale lateral carbon transport and CO_2 evasion in temperate stream catchments. *Biogeosciences*, *14*(21), 5003–5014.

Marchand, D., Prairie, Y. T., & Del Giorgio, P. A. (2009). Linking forest fires to lake metabolism and carbon dioxide emissions in the boreal region of Northern Québec. *Global Change Biology*, *15*(12), 2861–2873. https://doi.org/10.1111/j.1365-2486.2009.01979.x

Marshall, I., Schut, P., & Ballard, M. (1999). A National Ecological Framework for Canada: Attribute data. Technical report, Agriculture and Agri-Food Canada, Research Branch, Centre for Land and Biological Resources Research and Environment Canada, State of the Environment Directorate, Ecozone Analysis Branch, Ottawa/Hull.

Marx, A., Conrad, M., Aizinger, V., Prechtel, A., van Geldern, R., & Barth, J. A. C. (2018). Groundwater data improve modelling of headwater stream CO_2 outgassing with a stable DIC isotope approach. *Biogeosciences*, *15*(10), 3093–3106.

Marx, A., Dusek, J., Jankovec, J., Sanda, M., Vogel, T., van Geldern, R., … Barth, J. A. C. (2017). A review of CO_2 and associated carbon dynamics in headwater streams: A global perspective. *Reviews of Geophysics*, 1–26.

McEachern, P., Prepas, E. E., Gibson, J. J., & Dinsmore, W. P. (2000). Forest fire induced impacts on phosphorus, nitrogen, and chlorophyll a concentrations in boreal subarctic lakes of northern Alberta. *Canadian Journal of Fisheries and Aquatic Sciences*, *57*(S2), 73–81. https://doi.org/10.1139/f00-124

Miller, J. B., & Tans, P. P. (2003). Calculating isotopic fractionation from atmospheric measurements at various scales. *Tellus*, *Series B: Chemical and Physical Meteorology*, *55*(2), 207–214.

Natchimuthu, S., Wallin, M. B., Klemedtsson, L., & Bastviken, D. (2017). Spatio-temporal patterns of stream methane and carbon dioxide emissions in a hemiboreal catchment in Southwest Sweden. *Scientific Reports*, *7*(January), 39729.

O'Donnell, J. A., Jorgenson, M. T., Harden, J. W., McGuire, A. D., Kanevskiy, M. Z., & Wickland, K. P. (2012). The effects of permafrost thaw on soil hydrologic, thermal, and carbon dynamics in an Alaskan peatland. *Ecosystems*, *15*(2), 213–229.

O'Leary, M. H. (1988). Carbon isotopes in photosynthesis. *BioScience*, *38*(5), 328–336.

Olefeldt, D., Devito, K. J., & Turetsky, M. R. (2013). Sources and fate of terrestrial dissolved organic carbon in lakes of a Boreal Plains region recently affected by wildfire. *Biogeosciences*, *10*(10), 6247–6265.

Öquist, M. G., Wallin, M., Seibert, J., Bishop, K., & Laudon, H. (2009). Dissolved inorganic carbon export across the soil/stream interface and its fate in a boreal headwater stream. *Environmental Science & Technology*, *43*(19), 7364–7369. https://doi.org/10.1021/es900416h

Polsenaere, P., & Abril, G. (2012). Modelling CO_2 degassing from small acidic rivers using water pCO_2, DIC and δ^{13}C-DIC data. *Geochimica et Cosmochimica Acta*, *91*, 220–239.

Porter, C., Morin, P., Howat, I., Noh, M.-J., Bates, B., Peterman, K., …Bojesen, M. (2018). ArcticDEM, https://doi.org/10.7910/DVN/OHHUKH, Harvard Dataverse, V2, 2018-03-21.

Pries, C. E., Schuur, E. A., & Crummer, K. G. (2012). Holocene carbon stocks and carbon accumulation rates altered in soils undergoing permafrost thaw. *Ecosystems*, *15*(1), 162–173.

Quinton, W. L., Hayashi, M., & Chasmer, L. E. (2011). Permafrost-thaw-induced land-cover change in the Canadian subarctic: Implications for water resources. *Hydrological Processes*, *25*(1), 152–158. https://doi.org/10.1002/hyp.7894

Quinton, W. L., Hayashi, M., & Pietroniro, A. (2003). Connectivity and storage functions of channel fens and flat bogs in northern basins. *Hydrological Processes*, *17*(18), 3665–3684.

Rasilo, T., Hutchins, R. H., Ruiz-González, C., & del Giorgio, P. A. (2017). Transport and transformation of soil-derived CO_2, CH_4 and DOC sustain CO_2 supersaturation in small boreal streams. *Science of the Total Environment*, *579*, 902–912. https://doi.org/10.1016/j.scitotenv.2016.10.187

Raymond, P. A., Hartmann, J., Lauerwald, R., Sobek, S., McDonald, C., Hoover, M., … Guth, P. (2013). Global carbon dioxide emissions from inland waters. *Nature*, *503*(7476), 355–359.

Robinson, S. D., & Moore, T. R. (2000). The influence of permafrost and fire upon carbon accumulation in high boreal peatlands, Northwest Territories, Canada. *Arctic, Antarctic, and Alpine Research*, *32*(2), 155.

Rocher-Ros, G., Sponseller, R. A., Bergström, A.-K., Myrstener, M., & Giesler, R. (2019). Stream metabolism controls diel patterns and evasion of CO_2 in Arctic streams. *Global Change Biology*, https://doi.org/10.1111/gcb.14895

Rocher-Ros, G., Sponseller, R. A., Lidberg, W., Mörth, C., & Giesler, R. (2019). Landscape process domains drive patterns of CO_2 evasion from river networks. *Limnology and Oceanography Letters*, https://doi.org/10.1002/lol2.10108

Romeijn, P., Comer-Warner, S. A., Ullah, S., Hannah, D. M., & Krause, S. (2019). Streambed organic matter controls on carbon dioxide and methane emissions from streams. *Environmental Science and Technology*, *53*(5), 2364–2374.

Rouse, W. R., Douglas, M. S. V., Hecky, R. E., Hershey, A. E., Kling, G. W., Lesack, L., … Smol, J. P. (1997). Effects of climate change on the freshwaters of arctic and subarctic North America. *Hydrological Processes*, *11*(8), 873–902. https://doi.org/10.1002/(SICI)1099-1085(19970630)11:8<873::AID-HYP510>3.0.CO;2-6

Rumble, J. R., Lide, D. R., & Bruno, T. J. (2018). *CRC handbook of chemistry and physics*. Cleveland, OH: CRC Press.

Running, S., & Mu, Q. (2015). MOD17A3 MODIS/terra gross primary productivity yearly L4 global 1km SIN grid.

Schuur, E. A., McGuire, A. D., Schädel, C., Grosse, G., Harden, J. W., Hayes, D. J., … Vonk, J. E. (2015). Climate change and the permafrost carbon feedback. *Nature*, *520*(7546), 171–179.

Serikova, S., Pokrovsky, O. S., Ala-Aho, P., Kazantsev, V., Kirpotin, S. N., Kopysov, S. G., … Karlsson, J. (2018). High riverine CO_2 emissions at the permafrost boundary of Western Siberia. *Nature Geoscience*, *11*(11), 825–829.

Spence, C., Kokelj, S. V., Kokelj, S. A., McCluskie, M., & Hedstrom, N. (2015). Evidence of a change in water chemistry in Canada's subarctic associated with enhanced winter streamflow. *Journal of Geophysical Research: Biogeosciences*, *120*(1), 113–127.

Spence, C., & Woo, M. K. (2003). Hydrology of subarctic Canadian shield: Soil-filled valleys. *Journal of Hydrology*, *279*(1–4), 151–166.

Spencer, R. G. M., Mann, P. J., Dittmar, T., Eglinton, T. I., McIntyre, C., Holmes, R. M., … Stubbins, A. (2015). Detecting the signature of permafrost thaw in Arctic rivers. *Geophysical Research Letters*, *42*(8), 2830–2835.

Stackpoole, S. M., Butman, D. E., Clow, D. W., Verdin, K. L., Gaglioti, B. V., Genet, H., & Striegl, R. G. (2017). Inland waters and their role in the carbon cycle of Alaska. *Ecological Applications*, *27*(5), 1403–1420. https://doi.org/10.1002/eap.1552

Stanley, E. H., Casson, N. J., Christel, S. T., Crawford, J. T., Loken, L. C., & Oliver, S. K. (2016). The ecology of methane in streams and rivers: Patterns, controls, and global significance. *Ecological Monographs*, *86*(2), 146–171.

Statistics Canada. (2017). Human activity and the environment: Freshwater in Canada. (March 21):158.

Steinkamp, K., & Gruber, N. (2015). Decadal trends of ocean and land carbon fluxes from a regional joint ocean-atmosphere inversion. *Global Biogeochemical Cycles*, *29*(12), 2108–2126.

Striegl, R. G., Dornblaser, M. M., McDonald, C. P., Rover, J. R., & Stets, E. G. (2012). Carbon dioxide and methane emissions from the Yukon River system. *Global Biogeochemical Cycles*, *26*(4), n/a–n/a. https://doi.org/10.1029/2012GB004306

Tank, S. E., Lesack, L. F. W., & Hesslein, R. H. (2009). Northern delta lakes as summertime CO_2 absorbers within the Arctic landscape. *Ecosystems*, *12*(1), 144–157.

Tank, S. E., Olefeldt, D., Quinton, W. L., Spence, C., Dion, N., Ackley, C., … Hutchins, R. (2018). Fire in the Arctic: The effect of wildfire across diverse aquatic ecosystems of the Northwest Territories. *Polar Knowledge: Aqhaliat*, *1*(1), 31–38. https://doi.org/10.35298/pkc.2018.04

Tarnocai, C., Kettles, I., & Lacelle, B. (2011). Peatlands of Canada. Geological Survey of Canada, Open File 6561, 1 CD-ROM. https://doi.org/10.4095/288786

Teodoru, C. R., del Giorgio, P. A., Prairie, Y. T., & Camire, M. (2009). Patterns in pCO_2 in boreal streams and rivers of northern Quebec, Canada. *Global Biogeochemical Cycles*, *23*(2), GB2012–GB2012.

Tifafi, M., Guenet, B., & Hatté, C. (2018). Large differences in global and regional total soil carbon stock estimates based on soilgrids, HWSD, and NCSCD: Intercomparison and evaluation based on field data from USA, England, Wales, and France. *Global Biogeochemical Cycles*, 42–56. https://doi.org/10.1002/2017GB005678

Toohey, R. C., Herman-Mercer, N. M., Schuster, P. F., Mutter, E. A., & Koch, J. C. (2016). Multidecadal increases in the Yukon River Basin of chemical fluxes as indicators of changing flowpaths, groundwater, and permafrost. *Geophysical Research Letters*, *43*(23), 12,120–12,130.

Turner, D. P., Jacobson, A. R., Ritts, W. D., Wang, W. L., & Nemani, R. (2013). A large proportion of North American net ecosystem production is offset by emissions from harvested products, river/stream evasion, and biomass burning. *Global Change Biology*, *19*(11), 3516–3528. https://doi.org/10.1111/gcb.12313

Ulseth, A. J., Hall, R. O., Boix Canadell, M., Madinger, H. L., Niayifar, A., & Battin, T. J. (2019). Distinct air–water gas exchange regimes in low- and high-energy streams. *Nature Geoscience*, *12*(4), 259–263.

Venkiteswaran, J. J., Schiff, S. L., & Wallin, M. B. (2014). Large carbon dioxide fluxes from headwater boreal and sub-boreal streams. *PLoS ONE*, *9*(7), e101756.

Walker, X. J., Rogers, B. M., Baltzer, J. L., Cumming, S. G., Day, N. J., Goetz, S., … Mack, M. C. (2018). Cross-scale controls on carbon emissions from boreal forest megafires. *Global Change Biology*, *24*(9), 4251–4265. https://doi.org/10.1111/gcb.14287

Wallin, M. B., Campeau, A., Audet, J., Bastviken, D., Bishop, K., Kokic, J., … Grabs, T. (2018). Carbon dioxide and methane emissions of Swedish low-order streams-a national estimate and lessons learnt from more than a decade of observations. *Limnology and Oceanography Letters*, *3*(3), 156–167.

Wallin, M. B., Grabs, T., Buffam, I., Laudon, H., Ågren, A., Öquist, M. G., & Bishop, K. (2013). Evasion of CO_2 from streams – The dominant component of the carbon export through the aquatic conduit in a boreal landscape. *Global Change Biology*, *19*(3), 785–797. https://doi.org/10.1111/gcb.12083

Wallin, M. B., Löfgren, S., Erlandsson, M., & Bishop, K. (2014). Representative regional sampling of carbon dioxide and methane concentrations in hemiboreal headwater streams reveal underestimates in less systematic approaches. *Global Biogeochemical Cycles*, *28*(4), 465–479.

Wallin, M. B., Öquist, M. G., Buffam, I., Billett, M. F., Nisell, J., & Bishop, K. H. (2011). Spatiotemporal variability of the gas transfer coefficient (KCO_2) in boreal streams: Implications for large scale estimates of CO_2 evasion. *Global Biogeochemical Cycles*, *25*(3), 1–14.

Walvoord, M. A., & Kurylyk, B. L. (2016). Hydrologic impacts of thawing permafrost – A review. *Vadose Zone Journal*, *15*(6).

Wauthy, M., Rautio, M., Christoffersen, K. S., Forsström, L., Laurion, I., Mariash, H. L., … Vincent, W. F. (2018). Increasing dominance of terrigenous organic matter in circumpolar freshwaters due to permafrost thaw. *Limnology and Oceanography Letters*, *3*(3), 186–198. https://doi.org/10.1002/lol2.10063

Webb, J. R., Santos, I. R., Maher, D. T., & Finlay, K. (2018). The importance of aquatic carbon fluxes in net ecosystem carbon budgets: A catchment-scale review. *Ecosystems*, *22*, 508–527. https://doi.org/10.1007/s10021-018-0284-7

Zolkos, S., Tank, S. E., Striegl, R. G., & Kokelj, S. V. (2019). Thermokarst Effects on Carbon Dioxide and Methane Fluxes in Streams on the Peel Plateau (NWT, Canada). *Journal of Geophysical Research: Biogeosciences*, *124*, 1781–1798. https://doi.org/10.1029/2019JG005038

SUPPORTING INFORMATION

Additional supporting information may be found online in the Supporting Information section.

How to cite this article: Hutchins RHS, Tank SE, Olefeldt D, et al. Fluvial CO_2 and CH_4 patterns across wildfire-disturbed ecozones of subarctic Canada: Current status and implications for future change. *Glob Change Biol*. 2020;00:1–16. https://doi.org/10.1111/gcb.14960